

Application of vascular CFD for clinical evaluation of cerebral aneurysms

M.A. Castro^a, C.M. Putman^b, J.R. Cebal^{a,*}

^a*School of Computational Sciences, George Mason University, Fairfax, VA 22030, USA*

^b*Interventional Neuroradiology, Inova Fairfax Hospital, Falls Church, VA 22040, USA*

Abstract

The purpose of our study was to demonstrate the feasibility of using patient-specific 3-D rotational angiography (3DRA) image data from clinical studies to construct corresponding realistic patient-specific computational fluid dynamics (CFD) models of cerebral aneurysms. Using these models, the intra-aneurysmal flow patterns are characterized and their possible associations to the clinical history of aneurysmal rupture are explored. Finally, these models are used to analyze the alterations in the flow dynamics precipitated by endovascular procedures.

Keywords: Hemodynamics; Cerebral aneurysms; Rotational angiography; Stenting; Coiling

1. Introduction

Cerebral aneurysms are pathological dilatations of the arterial wall that frequently occur near arterial bifurcations in the circle of Willis [1]. The most serious consequence is rupture and intracranial hemorrhage into the subarachnoid space, which carries high mortality and morbidity rate [2]. Intra-aneurysmal hemodynamics is thought to be an important factor in the genesis, progression and rupture of cerebral aneurysms [3]. The purpose of our study was to construct patient-specific computational models of cerebral aneurysms for the analysis of the intra-aneurysmal flow patterns, to explore possible correlations to aneurysmal rupture, and to study the flow alterations produced by endovascular procedures.

2. Methods

2.1. Modeling pipeline

Realistic patient-specific models of cerebral aneurysm were constructed from 3DRA images using the following pipeline [4]: (1) filter the images to reduce noise (blur + sharpen operations), (2) seeded region growing

segmentation, (3) iso-surface extraction, (4) deformable model to match vessel boundaries, (5) surface smoothing, interactive truncation and extrusion of arterial branches, (6) finite element grid generation using advancing front technique, (7) numerical solution of the unsteady incompressible Navier-Stokes equations, and (8) post-processing and flow visualization. Pulsatile flow conditions were derived from phase-contrast magnetic resonance (PC-MR) measurements of blood flow velocity in the circle of Willis of a normal subject. Volumetric flow rate curves were obtained by integration of the velocity profile over the vessel cross section and fully developed Womersley velocity profiles were mapped to the inflow boundary.

2.2. Modeling aneurysms with multiple avenues of flow

Models of aneurysms with multiple feeding vessels were constructed from multiple 3DRA images obtained during contrast injection in each of the feeding vessels. The corresponding arterial trees are independently reconstructed. The images are co-registered using a manual rigid registration. The reconstructed models are then translated and rotated accordingly and merged using an adaptive voxelization technique [5]. Figure 1 illustrates the process and shows flow visualizations in an anterior communicating artery aneurysm.

* Corresponding author. Tel.: +1 703 993 4078; Fax: +1 703 993 4064; E-mail: jcebral@gmu.edu



Fig. 1. Construction of an anterior communicating artery aneurysm from two 3DRA images obtained by contrast injection in the left and right internal carotid arteries, respectively. Top row, left to right: volume rendering of right 3DRA image, volume rendering of left 3DRA image, co-registered images, co-registered images and vascular models, detail of vascular model of ACoA aneurysm, mean wall shear stress distribution, iso-velocity surface. Bottom row, left to right: right vascular model, left vascular model, co-registered vascular models, vascular model after merging, detail of the finite element grid, velocity distribution in two cuts through the aneurysm sac.

2.3. Modeling endovascular devices

The simulation of blood flow patterns in the presence of endovascular devices used to treat cerebral aneurysms such as coils and stents is a challenging problem due to the geometrical complexity of the devices. These devices operate by blocking the blood flow into the aneurysm, thus promoting clot formation and thrombosis, and reducing the risk of future rupture. Knowledge of the intra-aneurysmal hemodynamics after the device deployment is useful to evaluate, optimize and personalize the treatment options (e.g. selecting the optimal amount of coils for a given aneurysm). Preliminary simulations of blood flow dynamics in the presence of complex endovascular devices have been carried out using an adaptive embedding technique with very promising results [6]. The basic idea of this approach is to impose a wall boundary condition in the edges of the finite element grid that are intersected by the surface of the device. Coils and stents are modeled as a sequence of overlapping spheres that are then used to identify the edges of the mesh that are cut by the device. The mesh is adaptively refined in the proximity of the devices in order to resolve the flow features around the devices.

3. Results

3.1. Database of aneurysm models

A total of 65 patient-specific cerebral aneurysm models have been constructed. A database that contains anatomical images, reconstructed models, finite element grids, blood flow visualizations and clinical information has been created. Examples of aneurysm eight models and corresponding hemodynamic visualizations are

shown in Fig. 2 (from left to right: 3DRA images, anatomical model, peak pressure, mean wall shear stress, oscillatory shear index, velocity pattern). A large variety of flow patterns have been observed independently of aneurysm size, location and morphology type (i.e. lateral, bifurcation, terminal or fusiform).

3.2. Associations of hemodynamics and rupture

The aneurysms of the database were classified according to the complexity of the intraaneurysmal flow pattern and to the size of the flow impingement region. The distribution of rupture/unruptured aneurysms in each of these categories show interesting trends: most unruptured aneurysms have stable flow patterns, the majority of ruptured aneurysms have small impingement regions, and most aneurysms with large impingement regions are unruptured (see Fig. 3).

3.3. Endovascular procedures

Simulations of the endovascular treatment of a cerebral aneurysm with Guglielmi Detachable Coils (GDC) were performed. Simulated coils of different lengths (10 cm and 20 cm) were placed inside a patient-specific aneurysm model reconstructed from 3DRA images. Flow alterations produced by these two coils were calculated. Figure 4 shows the blockage of blood flow into the aneurysm after implantation of the coils.

4. Conclusions

An efficient pipeline for constructing patient-specific models of cerebral aneurysms has been developed. Methods to model cerebral aneurysms with multiple

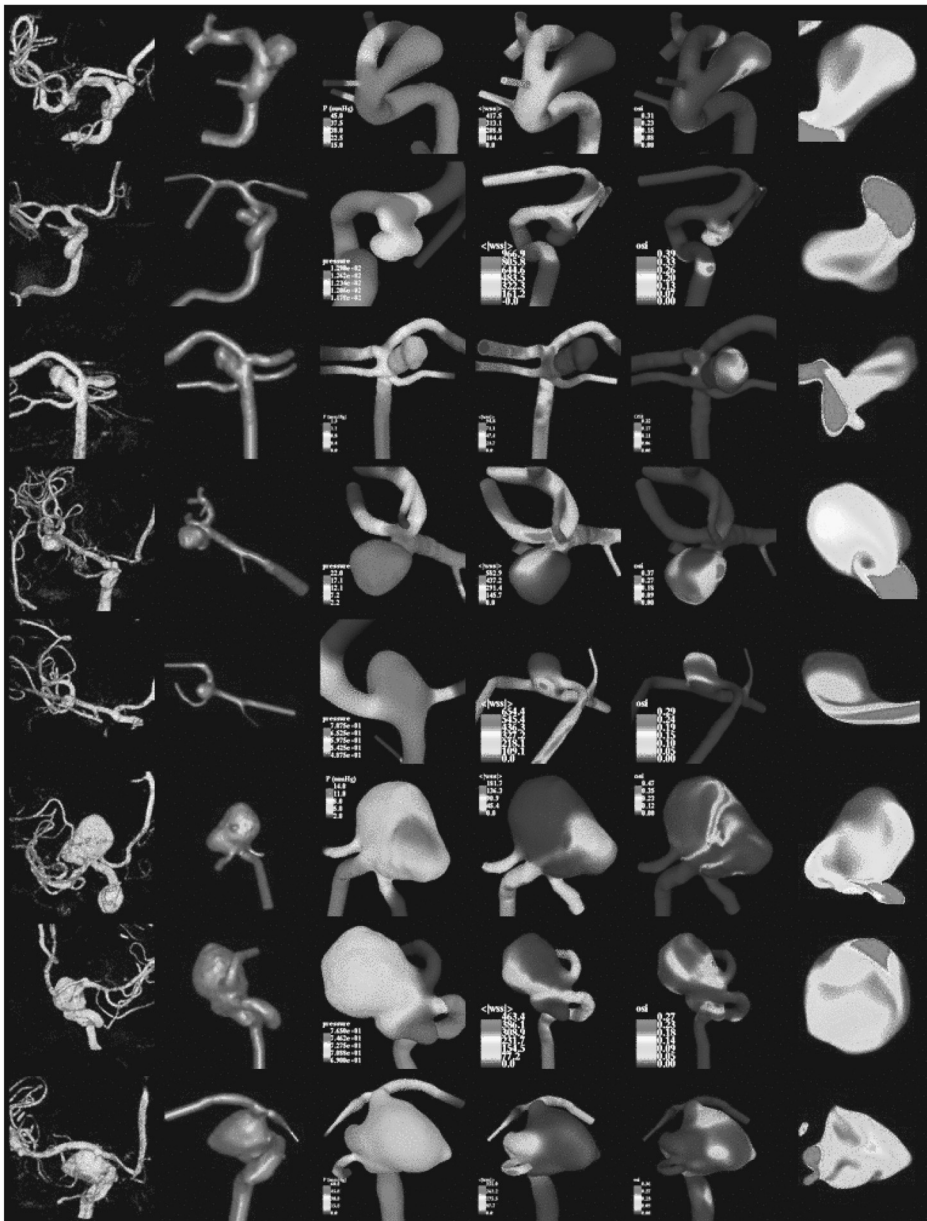


Fig. 2. Examples of eight patient-specific aneurysm models constructed from 3DRA images and visualizations of hemodynamic forces and intraaneurysmal flow patterns. Each row corresponds to a different aneurysm. Columns show: volume rendering of the 3DRA images, reconstructed vascular models, pressure distribution, mean wall shear stress, oscillatory shear index, and velocity pattern in a cut through the aneurysm sac.

feeding vessels have been developed. A database of patient-specific cerebral aneurysm models that can be interrogated to answer specific clinical questions has been implemented. In particular, the distributions of rupture/unruptured aneurysms with respect to the complexity of the flow pattern and size of the flow impingement region show interesting trends that can

potentially be used for clinical assessment of the risk of rupture. An adaptive embedding approach that tremendously simplifies the simulation of complex endovascular devices has been developed, making these techniques for the first time very attractive for clinical studies of endovascular interventions.

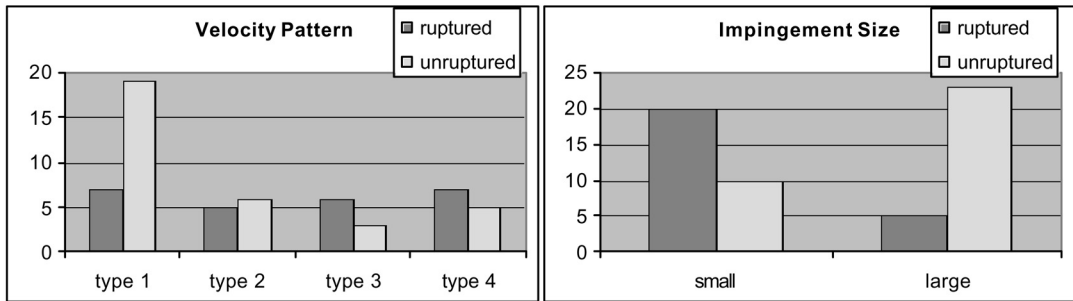


Fig. 3. Distribution of rupture/unruptured aneurysms with respect to the complexity and stability of the intraaneurysmal flow pattern (left) and size of the flow impingement region (right).

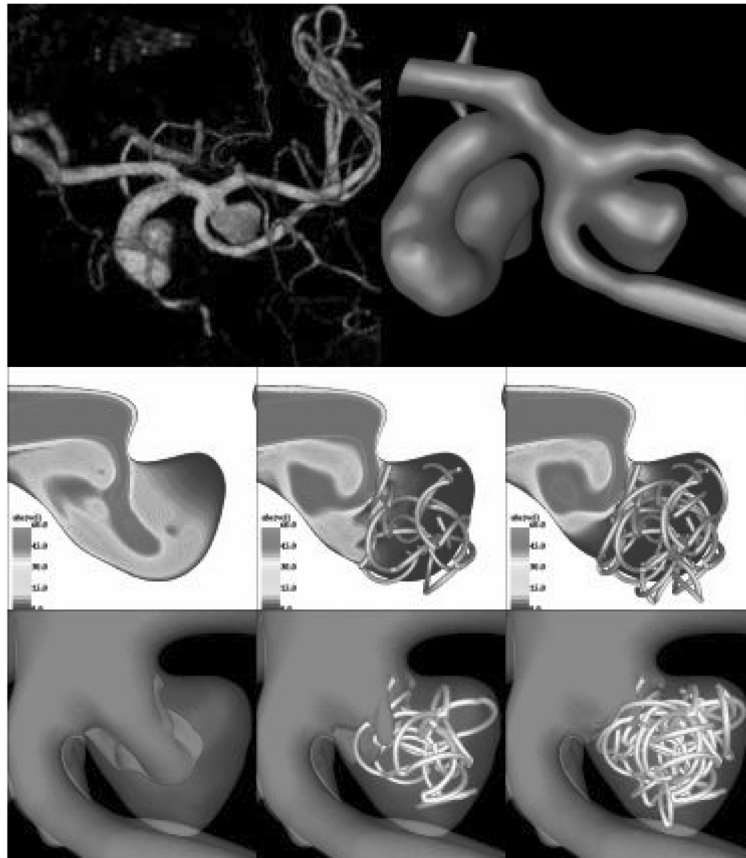


Fig. 4. Patient-specific simulation of the endovascular treatment of a cerebral aneurysm with coils of different sizes. Top row: volume rendering of 3DRA image (left) and reconstructed vascular model (right). Middle row: velocity pattern on a cut through the aneurysm sac before coiling (left), after coiling with a 10 cm coil (center) and with a 20 cm coil (right). Bottom row: iso-velocity surfaces before coiling (left), after coiling with a 10 cm coil (center) and with a 20 cm coil (right).

Acknowledgments

We thank Philips Medical Systems and Richard Kemkers for encouragement and technical support.

References

- [1] Nakatani H, Hashimoto N, Kang Y, et al. Cerebral blood flow patterns at major vessel bifurcations and aneurysms in rats. *J Neurosurgery* 1991;74:258–262.

- [2] Gonzalez CF, Choi YI, Ortega V, et al. Intracranial aneurysms: flow analysis of their origin and progression. *AJNR Am J Neuroradiol* 1992;13:181–188.
- [3] Gobin YP, Counard JL, Flaud P, et al. In vitro study of haemodynamics in a giant saccular aneurysm model: influence of flow dynamics in the parent vessel and effects of coil embolization. *Neuroradiology* 1994;36:530–536.
- [4] Cebal JR, Hernandez M, Frangi AF, Putman CM, Pergolizzi R, Burgess JE. Subject-specific modeling of intracranial aneurysms. *Proc SPIE Medical Imaging* 2004;5369:319–327.
- [5] Cebal JR, Löhner R, Choyke PL, Yim PJ. Merging of intersecting triangulations for finite element modeling. *J Biomech* 2001;34:815–819.
- [6] Cebal JR, Löhner R. Efficient simulation of blood flow past complex endovascular devices using an adaptive embedding technique. *IEEE TMI*, 2004 (in press).